Partitioning 3D Surface Meshes Using Watershed Segmentation

Alan P. Mangan and Ross T. Whitaker

Abstract—This paper describes a method for partitioning 3D surface meshes into useful segments. The proposed method generalizes morphological watersheds, an image segmentation technique, to 3D surfaces. This surface segmentation uses the total curvature of the surface as an indication of region boundaries. The surface is segmented into patches, where each patch has a relatively consistent curvature throughout, and is bounded by areas of higher, or drastically different, curvature. This algorithm has applications for a variety of important problems in visualization and geometrical modeling including 3D feature extraction, mesh reduction, texture mapping 3D surfaces, and computer aided design.

Index Terms—Surfaces, surface segmentation, watershed algorithm, curvature-based methods.

1 Introduction

Consider a 3D surface mesh. It can be described as a set of faces that share edges, or a set of vertices that are connected to neighboring vertices by edges. In many cases, such meshes have no explicit higher-level structure; they exist simply as a collection of connected polygons—a *bucket of polygons*. One way to impose a higher level structure on such a mesh is to partition it into a set of connected pieces, which themselves have relationships to other pieces. Presumably, the pieces should represent something about the underlying structure of the object itself—the *semantic* meaning of the object's parts and subparts. However, when no structure, other than the local connectedness of the polygons, is specified, any algorithm seeking to partition such meshes must infer some structure from the local shape (e.g., geometry) of the mesh itself. We call the problem of partitioning a 3D surface mesh into meaningful, connected pieces the *mesh segmentation problem*. By meaningful, we propose that the relative size and organization of the segmented regions must be relevant to the application at hand. This problem bears a strong resemblance to the partitioning of images in image processing and computer vision. The mesh segmentation problem, like the image segmentation problem, is not well posed; solutions are often application specific, depending quite heavily on one's definition of "meaningful."

The 3D mesh segmentation method we present here is based on the concept of "catchment basins" or "watersheds," which has been used previously in image segmentation [1]. For images, the algorithm operates on a height function (usually the gradient magnitude of the input image), which is defined over the image domain, typically some compact, continuous subset of $\Re^2$. This work presents a generaliztion of the watershed method in order to segment 3D surface meshes. For the case of 3D meshes, the height function is defined over the mesh itself. One such height function is the total curvature of the surface (or some approximation thereof) defined at each vertex of the mesh.

There are several reasons why one would want to segment a 3D mesh. Generally, datasets are more manageable at the higher level of abstraction that such a partitioning affords. There are also some specific applications that could benefit from such a capability. One example is mesh reduction [2], [3]. Effective *mesh reduction* algorithms can dramatically reduce the amount of data in a 3D mesh while maintaining, to a certain degree, the fidelity of the surface. Most mesh reduction algorithms operate on the data as a whole, with individual vertices or faces treated solely with respect to their immediate neighbors. However, we propose mesh segmentation as a preprocessing step that could indicate to subsequent mesh reduction algorithms that they should preserve distinct parts of objects. Results in this paper will show that a mesh segmentation technique that relies on surface curvature can help preserve edges, creases, and other fine details during subsequent mesh reduction.

A related application is the reparameterization of irregularly connected meshes in order to apply successive reduction or refinement algorithms. For instance, Lee et al. [4] describe a technique that generates a hierarchy of regular meshes from irregularly connected meshes of arbitrary topology. This process can preserve designated vertices and edges that are important to the structure of the object. The generation of such *special* structures could require a great deal of user input. Alternatively, those structures could be generated automatically using a mesh segmentation algorithm such as the one described in this paper.

Another application of mesh segmentation is the fitting of higher-order models to polygonal meshes. Because the proposed segmentation method breaks the surface into regions comprised of relatively consistent curvature (and bounded by high curvature), the geometry of the regions

- *A.P. Mangan is with Creare Inc., PO Box 71, Hanover, NH 03755. E-mail: spm@creare.com.*
- *R.T. Whitaker is with the Department of Electrical Engineering, University of Tennessee, Knoxvill, TN 37996-2100. E-mail: rtw@utk.edu.*

For information on obtaining reprints of this article, please send e-mail to: tvcg@computer.org, and reference IEEECS Log Number 109330.

tends to be homogeneous. Rather than using mesh reduction to decrease the complexity of the surface data, large-scale structures, such as planes, quadrics, superquadrics, or B-splines, can be used to *model* these areas. For example, indoor scenes, or those consisting primarily of artificial objects, tend to have more planar and angular surfaces than those occurring in nature. In such cases, a higher-level modeling scheme consisting of geometric primitives might be appropriate. Outdoor scenes, on the other hand, are typically less organized and might be better modeled using algebraic structures or B-splines. Each region of the surface, having been segmented and classified according to surface type, could have a model assigned to it.

A further use of mesh partitioning is the modification of existing 3D CAD models. As 3D models become more ubiquitous and available from a large number of difference sources (e.g., through the internet), interesting models tend to be in formats that are inappropriate for certain applications. In such cases, people using these models will be interested in modifying them to suit their own needs. Using the proposed surface segmentation scheme, a user could impose some structure on such models (perhaps after scan converting or tiling them). The model can then be modified on a region-by-region basis, making it easier to concentrate on a specific portion of the design. Sections and subassemblies of the model can be isolated for modification. Portions of structures in this manner could also be imported from existing parts databases and reused.

Another application of mesh segmentation is feature detection. In some applications, such as medical imaging, one would like to locate points or lines on a surface that could serve as landmarks for comparing or aligning it with other surfaces. These landmarks should be relatively insensitive to noise and invariant to certain kinds of geometric transformations. One way to establish a set of landmarks is to use the boundaries of segments, particularly when those boundaries have some geometric interpretation, as is the case with the methods proposed in this paper.

The remainder of the paper proceeds as follows: The next section describes some aspects of the literature that are related to the proposed algorithm. Section 3 presents the watershed algorithm in the context of images and then the generalization to 3D meshes. After completion of the watershed segmentation, it is also necessary to perform an additional step of region merging in order to avoid over-segmentation, that is, to control the level of detail in the segmentation. That section also describes the region merging process and Section 4 explains how surface curvature is computed, both directly from isosurfaces of volumes and from vertex-list type geometric models. Section 5 presents results and analyzes the performance of the algorithm. It describes the capability of the algorithm to segment simple surfaces, the effects of added noise, and the performance of the algorithm when segmenting complex surfaces.

2 Related Work

There are several somewhat diverse areas of research that are relevant to this work. One area is the problem in computational geometry of attempting to divide polyhedra into convex components. Another area is the detection of geometric features, namely creases, on continuous surfaces. Another related area is the problem of surface classification from range data. Last, there is that part of image processing which applies morphological watersheds to image segmentation.

In the field of computational geometry, researchers [5], [6] have addressed the problem of dividing polyhedra into collections of convex pieces. Of course, the individual faces are each convex, but if one considers the optimal partitioning (e.g., smallest number of pieces), the problem is NP-complete [7]. Several researchers have proposed reasonable algorithms for obtaining *good* solutions. Unlike the problem addressed in this paper, the convex-decomposition problem is purely geometric and is well posed; state-of-the-art research focuses on developing efficient algorithms. Such a convex decomposition is useful for algorithms that explicitly depend on convex objects (such as certain 3D rendering algorithms or collision detection), but less useful for applications that are trying to get a part-subpart decomposition that is related to the underlying structure of the object. For instance, a convex decomposition must partition hyperbolic regions into their constituent flat faces—a partitioning which has little to do with the overall shape of an object (e.g., a torus) that happens to contain such regions. Fig. 1a shows an example of how two objects joined by a smooth fillet create a hyperbolic region. In this example, a convex decomposition will produce less than adequate results (Fig. 1b) and will, without heuristics, partition the hyperbolic region into its constituent (atomic) planar faces. In this same example, a curvature-based segmentation could, in principle, partition the surface along meaningful, intuitive boundaries (e.g., Fig. 1c) that divide the faces of objects and break the protrusion from the main body of the larger object.

Another related problem is the detection of certain kinds of geometric features on surfaces. The detection of such features can be important in comparing, registering, and analyzing shapes. Perhaps the most closely related idea is "ridge detection" on surfaces [8], [9]. Because ridges are usually assumed to be maxima in curvature, the operators required to detect them rely upon third- and fourth-order derivatives. Such derivatives are very sensitive to noise, requiring some robust approximation, such as a polynomial fit or a low-pass filter—both of which tend to distort the shapes of the features being detected. For this reason, there are few examples in the literature that make practical use of such surface ridges for segmenting 3D meshes. Our method does not attempt to explicitly locate ridges. Rather, the surface is segmented into *patches* bounded by regions where sharp differences in surface normal create a boundary. Although these boundaries do occur at places of high curvature, the watershed algorithm makes no attempt to explicitly locate these edges/ridges and does not require derivatives beyond second-order (first-order derivatives of the normal).

Surface segmentation is also related to the problem of *surface classification*. Extracting surface patches by identifying individual surface elements as certain types has played

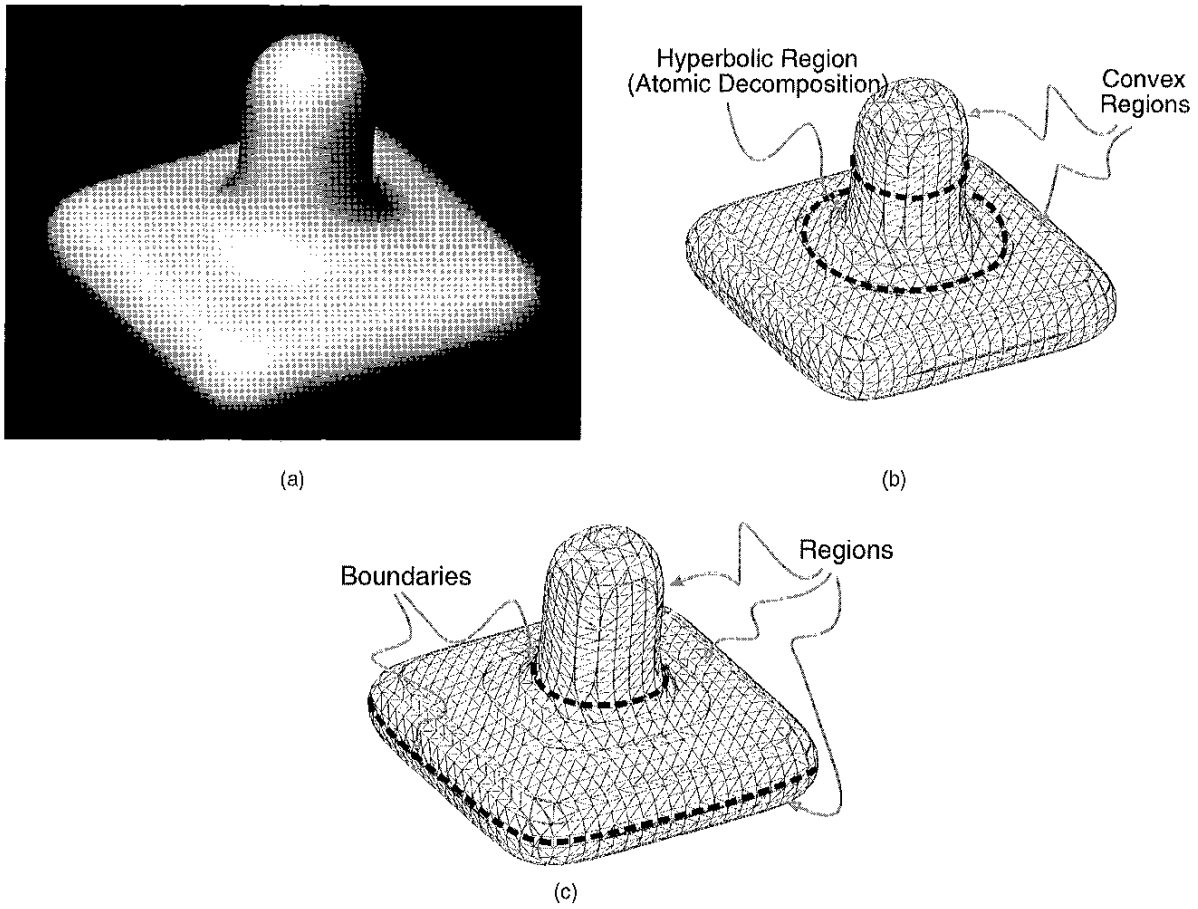

Fig. 1. Convex decomposition. (a) A protusion is joined to a larger object by a smooth fillet, creating a hyperbolic region. (b) A convex decomposition divides the surface along lines that are not perceptually meaningful while decomposing the hyperbolic region into its constituent planar faces. (c) A curvature-based method could, in principle, partition the surface along lines that distinguish individual faces and part/subpart boundaries.

an important role in high-order systems, such as 3D recognition. For instance, Fisher et al. [10] address the problem of extracting surface patches from range data with the goal of constructing CAD models. Their method uses a curvature-based surface classification algorithm to perform segmentation. Faugeras and Hebert [11] also approach the problem of 3D segmentation from a scene recognition viewpoint. They perform geometric matching between primitive surfaces (mainly planar, although the more general case of quadrics is discussed). Besl [12] proposes using the mean and Gaussian curvatures in segmenting and classifying surfaces by type. These approaches are based on range data, which is always a *graph*—a special class of 3D surfaces—whereas the method we propose is suited to the more general class of 3D surfaces. We make use of the mean and Gaussian curvatures in calculating the total curvature, but do not explicitly attempt to classify any particular surface region. Rather than use only local differential structure to classify regions into one of several simple types, we partition regions based on the homogeneity of the surface normal, combining local information at many points to form a region. Thus, the proposed algorithm is broadly applicable to many types of 3D surfaces and does not rely upon the classification and matching of any type of underlying geometric primitive.

Similarly, the computer vision literature shows examples of the application of image segmentation techniques to surfaces, such as range maps, that are height functions, i.e., $z = f(x, y)$, defined on a rectilinear grid [13], [14]. These are essentially image segmentation techniques that include some analysis of the local image surface structure. The goal of this paper is to describe the generalization of one such algorithm to a full 3D surface and demonstrate its effectiveness in addressing several problems in computer graphics and vision.

The problem of segmentation is central to image processing and computer vision and has been an area of active research for more than 30 years. Watersheds for image segmentation are described in the classic work of Serra [1] on mathematical morphology. Since that time, they have found a wide range of applications including medical imaging [15], [16], shape analysis [17], and range-image segmentation [14]. Koënderink and Van Doorn [18] argue for watersheds as a method of detecting "ridges" as an alternative to constructing detectors that rely on higher-order derivatives. Eberly [9] gives a nice overview of that

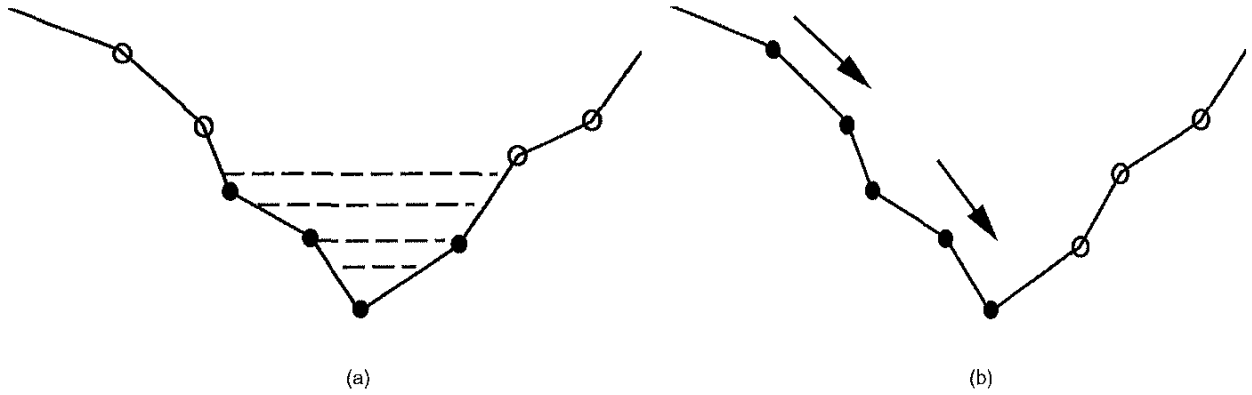

Fig. 2. Watershed strategies. (a) The bottom-up approach to finding catchment basins is to start at a local minimum and incrementally flood the region until it connect to its neighbors. (b) The top-down approach is to place a token at a point and move the token along a steepest descent until it reaches a minimum.

debate and also discusses the use of scalar functions defined on manifolds as a means of detecting ridges.

In this paper, we use the notion of defining a scalar function on a manifold (in this case, the scalar function is surface curvature and the manifold is a 3D surface mesh), but we apply morphological watersheds as a means of segmenting that surface. The algorithm we use traces points on the surface "down" to local minima, as in [15]. The difference with the proposed algorithm and previous work is the generalization of morphological watersheds to a 3D polygonal mesh and the use of a depth measure to reduce insignificant regions.

3 Watershed Algorithm

This section describes the strategy used in the watershed algorithm and the specifics of the implementation. The image processing version of the algorithm is first briefly introduced and an example of image segmentation using this approach is given. The generalization of the algorithm from a 2D rectilinear grid to an arbitrary surface with well-defined neighbor connectivity is then presented.

3.1 Watersheds in Image Processing

The watershed algorithm derives its name from the manner in which regions are segmented into *catchment basins*. Let $f(x, y) : U \rightarrow \Re$ be a continuous height function defined over the image domain $U \subset \Re^2$. A catchment basin is the set of points whose path of steepest descent terminates in the same local minimum of f. The choice of height function depends on the application; the basic algorithm is independent of the height function. For instance, one might choose the original image in order to locate blobs (light and dark regions), as in [15], or one could choose the gradient magnitude of the image in order to locate regions that are relatively homogeneous [14].

After locating these minima in f, there are two strategies for associating catchment basins with these minima. One strategy is to incrementally "flood" the regions surrounding these minima, keeping track of the places where flood regions touch [1], [14]. This method typically requires one to discretize the range (or gray levels) of f, thus limiting the contrast resolution of the resulting segmentation. If the domain of f is discrete (as is usually the case), an alternative is to take each point in U and *flow* downward until one encounters a minimum or a point which has already been associated with a minimum (see Fig. 2). The connectivity of the points in U depends on the discretization, but, with rectilinear grids, four connectivity is usually sufficient. If labels are updated incrementally, the computation time is proportional to the number of points in the image times the connectivity. For 3D mesh segmentation, we have chosen the latter approach, which we call the *top-down* approach, because it is better suited for the irregular topology of the 3D mesh. In both algorithms, there are special cases that must be considered. For instance, there may be flat regions, *plateaus*, where there is no downhill direction across neighboring vertices. Such details are discussed in the sections that follow.

An example of the application of the watershed algorithm to images serves as a good starting point for the extension to 3D meshes. Fig. 13 shows an input image, the gradient magnitude of that image (which serves as f), and the segmentation that results from following pixels (using four-connected neighbors) through a steepest descent to the local minima.

3.2 Extension to 3D

Our goal is to extend this algorithm to a 3D mesh consisting of connected vertices, each of which has a value of f and a set of connections to neighboring vertices, as displayed in Fig. 3. Let X be the set of all vertices in the mesh. For each $x_i \subset X$, there is a connected neighborhood of x_i, $N_i \subseteq X$. Such a neighborhood is shown in Fig. 3. In the image processing case, we traverse a 2D network of points where each point's neighbors are defined by a rectilinear grid. In the case of a surface mesh, we move tokens around a network of points in 3D, where each point's neighbors vary, depending upon the mesh geometry and connectivity at that point. A token moves from one vertex to its neighbor of

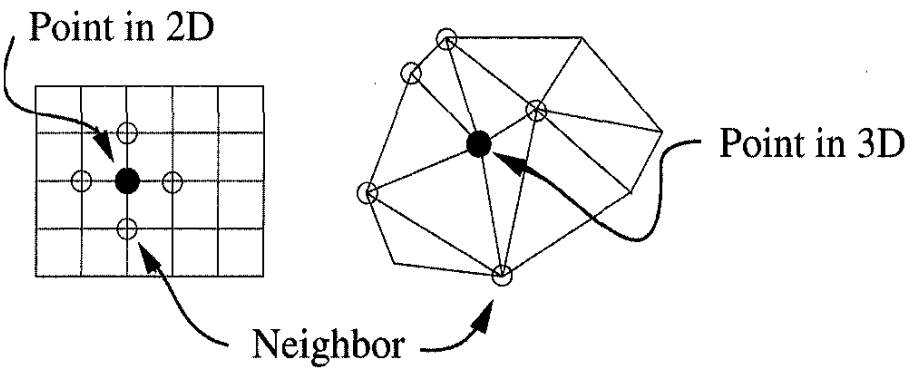

Fig. 3. Neighborhood relationships for a 2D rectilinear grid (left) and a 3D mesh of connected vertices (right).

lowest value until it reaches a minimum (which it must, by definition). The 3D positions of the vertices are not relevant to this process; only the topology of the vertices and the values of the height function affect the formation of catchment basins. Thus, the shape of the surface affects the segmentation via the height function.

Therefore, the steps of the watershed segmentation algorithm are as follows:

1. Compute the curvature (or some other height function) at each vertex.
2. Find the local minima and assign each a unique label.
3. Find each flat area and classify it as a minimum or a plateau.
4. Loop through plateaus and allow each one to descend until a labeled region is encountered.
5. Allow all remaining unlabeled vertices to similarly descend and join to labeled regions.
6. Merge regions whose watershed depth is below a preset threshold.

The following sections describe in more detail the specific steps for computing the watershed segmentation.

The input to the watershed method is a surface mesh and whatever additional information (e.g., surface normals) is necessary to calculate the curvature at each vertex. The algorithm then segments this mesh, using the curvature as the height function f. Thus, the first step of the segmentation is the calculation of curvature at each vertex on the surface. The method for calculating curvature should depend on the application and type of input data available. The methods for curvature calculation used in this work are discussed in Section 4. The watershed algorithm, per se, is independent of the type of curvature used.

3.3 Initial Labeling

Once the curvature (height function) is defined on the surface mesh, the watershed method labels all of the local minima, i.e., those vertices with curvature lower than that of all of their neighbors, as in Fig. 4a. Each minimum then serves as the initial basis for a surface segment, i.e., a distinct region on the surface formed during the descent of vertices along their paths of steepest descent. Next, flat regions are found. These are one of two types as shown in Fig. 4b; either flat plateaus or flat minima. Flat plateaus are defined as those flat regions that have any vertices adjacent to their borders with a lower curvature than that of the plateau itself. A variation of the algorithm is to define an additional type of flat region; the *flat maximum*, which has all adjacent points lower than itself. These maxima may also be used as indicators of borders between regions. We treat these maxima, if present, in the same manner as flat plateaus and do not explicitly define any points as border vertices. Flat minima have all adjacent vertices with higher curvatures than themselves. These minima are labeled and treated in the same manner as local single-vertex minima. Once all flat regions are found and classified, a descent is made from each of the flat plateaus until a labeled region is encountered. The curvatures of all adjacent vertices of the plateau are examined and the descent from the plateau begins at that vertex with the lowest curvature.

3.4 Descent

The process of associating points together into catchment basins is what gives this method the name "watershed." Imagine a drop of water placed at the starting vertex, flowing downhill on the height function, i.e., toward the point of lowest curvature. The drop, or token, follows the path of gradient descent, and each vertex it encounters on its path "downward" is labeled with the same identifying label as the first labeled vertex it encounters, as shown in Fig. 2b. This token moves all of the way to a local (labeled) minimum or hits a labeled vertex that has already been associated with a minimum. Initially, descent is made from flat plateaus, followed by the remaining unlabeled vertices on the surface. The plateau and its path of descent are then labeled and joined to the region finally hit during the descent. If another flat plateau is encountered, then the two are joined and the resulting plateau will later descend in turn until a minimum is encountered. The plateaus are indexed, and joined as necessary, so that a token, upon reaching a plateau, can move through it in one step and continue its descent. The next step is to allow all other unlabeled vertices to similarly descend until they hit a labeled region, then label them and join them to that region.

3.5 Region Merging

The final step of labeling each vertex according to its associated minimum produces a segmented mesh. However, the watershed, as it stands, is sensitive to even the

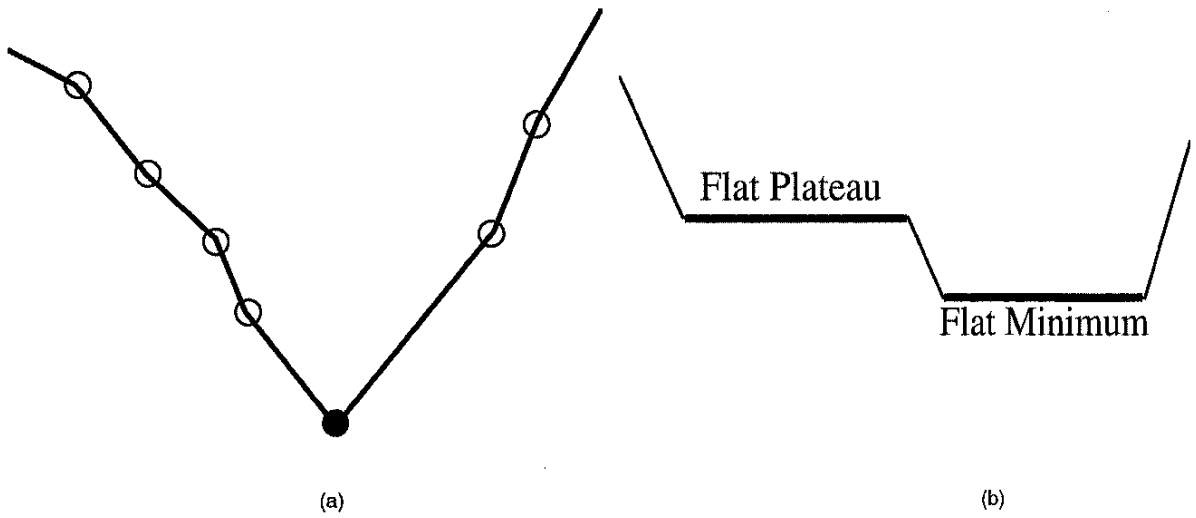

Fig. 4. Initial labeling. (a) Labeling of local minima and (b) classification of flat regions.

smallest fluctuations in surface shape—every local minimum of curvature establishes its own region. Leaving the surface in this state can yield a solution with regions that are too small and numerous to be useful (as shown in Fig. 10). It is necessary to merge the regions together in order to obtain reasonable results. The strategy is to use a saliency measure and the structure of the catchment basins to define a merging process.

There are a variety of possibilities for metrics that indicate insignificant regions, but the watershed algorithm itself gives a fairly reliable metric for determining the saliency of a segment. This metric is the greatest depth of water that a segment can hold before it "spills over" into one of its neighbors. Regions that are "shallow" are relatively constant in curvature, i.e., their boundaries have a curvature which is not significantly greater than the flattest part of that region. The watershed depth can be calculated as the difference between the point in the region with the overall lowest curvature (the local minimum) and the vertex along the region's boundary with the lowest curvature of all other boundary vertices, as in Fig. 5. This is the depth of water that the region can hold before it begins to overflow its boundary.

In calculating the lowest boundary point of a segment, it may be necessary to take into account those vertices immediately past the current region's boundary. This is a side effect of the discrete nature of the grid; because the watershed algorithm labels all vertices as being in one region or another, even though segments are separated by a single ridge of vertices which have downhill neighbors that flow into two separate catchment basins. These ridge vertices determine the minimum watershed depth. Notice that, in Fig. 5, the depth is found using such a vertex, vertex A. If the depth had merely been calculated using the vertex with the lowest curvature belonging to the current region, then vertex B would have been used, resulting in an incorrect, lower depth.

The region merging algorithm is as follows:

1. For each region, find its lowest point, neighbors, and lowest boundary point with each neighbor.
2. Find depth of region, the difference between the lowest point to lowest boundary point.
3. If depth is below a predefined threshold, merge this region to region adjacent to lowest boundary point and update new region's information accordingly.
4. Repeat until no regions exist that are below the minimum depth.

Once the depths of all regions are computed, those regions below the depth threshold are merged with their neighbors. In this manner, adjacent regions, at least one of which has a shallow depth, as in Fig. 6, are combined together. This drives the solution away from being oversegmented toward a more useful result. This merging process can be done very efficiently using the appropriate data structures and keeping a lookup table of merged regions. Several pieces of information must be tabulated for each region. The vertex with the lowest curvature for the region is found and used to later estimate the depth of the region. The boundary of the region is found and, from this, all neighboring regions are determined. For each neighbor B, the boundary vertex of the current region A adjacent to B with the lowest curvature is also found. From these boundary vertices, the lowest (in terms of curvature) boundary vertex of the region is then calculated. With this information, available region merging can then proceed.

When a shallow region is identified, the neighboring region into which the lowest boundary vertex would flow during descent is selected as that one with which to merge. This resolves any ambiguity that might arise in the case of there being more than one neighboring region adjacent to the lowest boundary vertex. For implementation purposes,

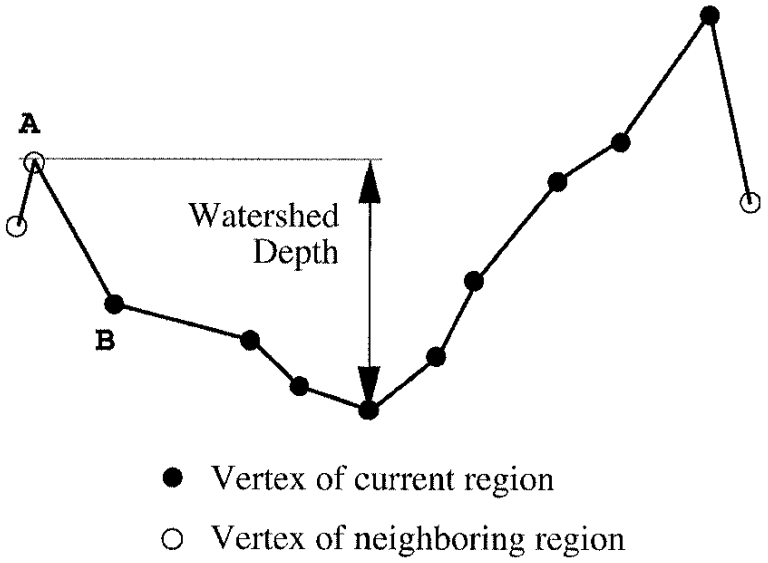

Fig. 5. Defining the depth of a region based on its lowest vertex and lowest boundary vertex.

rather than relabeling all of the region's vertices with the label of the neighboring region it just merged with, a pointer is set for the region indicating with which region it is merged. The pointers of all other regions merged with this one are also updated to reflect the new region with which they are now merged.

When merging regions, one must also update the information of the new region regarding lowest vertex, lowest boundary vertex, and neighbors. Comparing and changing the lowest curvature vertex is straightforward; adjusting the neighbor information of this new region is somewhat more complicated. All of the current region's neighbors need to be added as neighbors of the new region unless they themselves have been merged with the new region previously. The current region, and all other regions in turn merged with it, are then removed from the new region's list of neighbors. The boundary vertices associated with these neighbors also are removed from their respective lists. The new lowest boundary vertex is next recalculated, necessary in case the region associated with the previous lowest boundary vertex. The regions are merged in this manner according to Fig. 7. Once this information is updated, the new lowest boundary vertex has to be calculated and set. This merging procedure is repeated, cycling through all of the regions consecutively until no further regions are within the preset depth threshold. At this point, the watershed algorithm is complete.

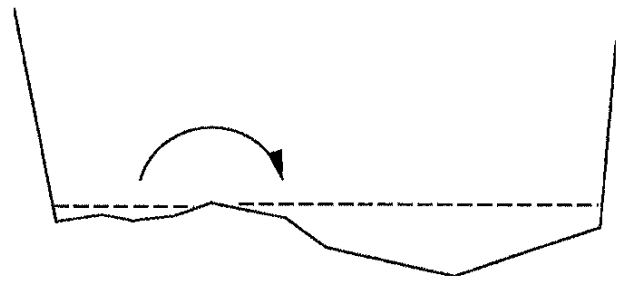

Fig. 6. Merging adjacent regions with shallow depths.

This basic strategy can be extended to incorporate other measures of saliency. Another *natural* measure is to compute the volume of the watershed (i.e., average depth times area), which would favor larger regions over smaller ones. One could also bring other information into this metric, such as triangle coloring or texture coordinates. We have experimented with area-based metrics and found that they penalize small areas too aggressively, which produces inferior results for the examples we have considered. The development, implementation, and verification of other saliency measures is an area for future work.

4 Curvature Calculation

The calculation of curvature depends on the type of data used and the level of noise in that data. In this work, we consider two different types of input: volumes whose voxels represent the value of some implicit function and simple surface meshes consisting of only vertices and triangles. In the former case, we can use the volume data itself to directly compute accurate estimates of the curvature of the embedded surface. Given a polygonal mesh (without an embedding) as input, there are several possibilities for discrete approximations to surface curvature. One approximation is the angle between the faces that are adjacent to a vertex. Another option is the norm of the covariance of the surface normals or edges that are adjacent to that vertex.

4.1 Isosurface Curvature

In the case of volumes, we are segmenting meshes corresponding to isosurfaces. The meshes are generated using the marching cubes algorithm [19]. Therefore, we can compute the curvature of the isosurface using the values of the volume itself as the surface is extracted. This provides a slightly more accurate estimate of the surface curvature than that obtained using the faces that

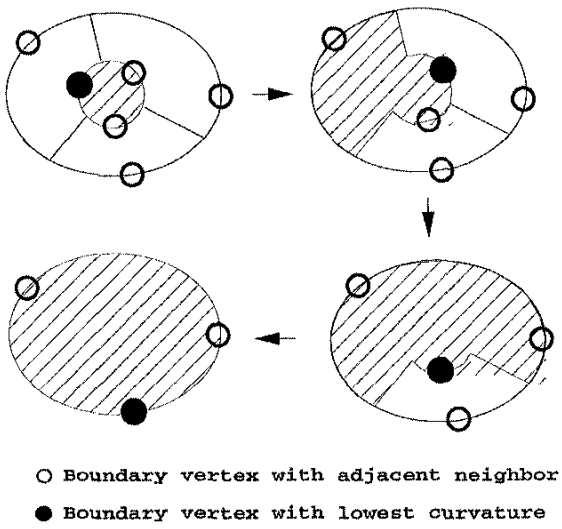

Fig. 7. Region merging. As each new region is added to the current region, indicated by the shaded area, its list of neighbors and associated boundary vertices needs to be updated accordingly.

are generated from the marching cubes algorithm. For the magnitude of the curvature, we use the *deviation from flatness* [20], which is defined to be the Euclidean norm of the shape tensor. The mean, H, and Gaussian curvature,K, are first found from [21],

$$H = \frac{\begin{pmatrix} \phi_x^2(\phi_{yy}+\phi_{zz}) + \phi_y^2(\phi_{xx}+\phi_{zz}) \\ +\phi_z^2(\phi_{xx}+\phi_{yy}) - 2\phi_x\phi_y\phi_{xy} - 2\phi_z\phi_x\phi_{xz} - 2\phi_y\phi_z\phi_{yz} \end{pmatrix}}{(\phi_x^2+\phi_y^2+\phi_z^2)^{3/2}} \tag{1}$$

$$K = -\frac{\begin{pmatrix} \phi_x^2(\phi_{yy}\phi_{zz}-\phi_{yz}\phi_{yz}) + \phi_y^2(\phi_{xx}\phi_{zz}-\phi_{xz}\phi_{xz}) \\ +\phi_z^2(\phi_{xx}\phi_{yy}-\phi_{xy}\phi_{xy}) + 2(\phi_x\phi_y(\phi_{xz}\phi_{yz}-\phi_{xy}\phi_{zz}) \\ +\phi_y\phi_z(\phi_{xy}\phi_{xz}-\phi_{yz}\phi_{xx}) + \phi_z\phi_x(\phi_{xy}\phi_{yz}-\phi_{xz}\phi_{yy})) \end{pmatrix}}{(\phi_x^2+\phi_y^2+\phi_z^2)^2}, \tag{2}$$

where ϕ represents the value of the implicit function at a given point in the volume. The total curvature, D, is then calculated using:

$$D = \sqrt{4H^2 - 2K^2}. \tag{3}$$

When computing the curvature values, we sometimes apply a threshold to the curvature, as shown in Fig. 8. This step is performed so that relatively flat areas where the curvature is extremely low throughout will be classified as exactly flat, easing the computational burden during later processing. This threshold does not have a significant affect on the final result because such shallow watersheds would be merged in the last part of our algorithm, as discussed in Section 3.5. Once this threshold has been applied, the watershed algorithm proper can begin.

4.2 Surface Mesh Curvature

There are several possibilities for finding the curvature of surfaces represented by polygonal meshes. We have

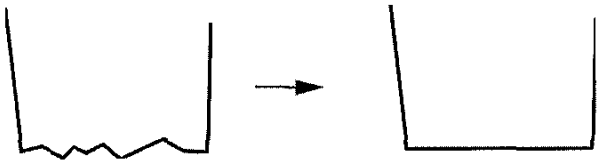

Fig. 8. Thresholding the total curvature.

experimented with two different approaches and achieved varying degrees of success for each. The first method uses the angles between the faces of the triangles to determine the curvature. The second uses the norm of the covariance of the surface normals adjacent to the vertex in question. The latter method proved to be the most successful because it is less sensitive to noise and it averages across faces that are composed simply of pairs of coplanar triangles.

To find the covariance matrix, the variance and covariance in all three cardinal directions must first be found. The variance and covariance are found from:

$$\sigma_{aa}^2 = \frac{1}{N}\sum_{t=0}^{N}(a_t - \bar{a})^2 \tag{4}$$

$$\sigma_{ab}^2 = \frac{1}{N}\sum_{t=0}^{N}(a_t - \bar{a})(b_t - \bar{b}) \tag{5}$$

$$a \in \{x, y, z\} \quad b \in \{x, y, z\}. \tag{6}$$

N represents the number of triangles associated with this vertex and $[x_t \quad y_t \quad z_t]$ are the components of the normal for triangle t. Also, $\sigma_{ab} = \sigma_{ba}$. The curvature, D, is then set equal to the norm of the covariance matrix, C;

$$D = \|C\| \qquad C = \begin{bmatrix} \sigma_{xx} & \sigma_{xy} & \sigma_{xz} \\ \sigma_{yx} & \sigma_{yy} & \sigma_{yz} \\ \sigma_{zx} & \sigma_{zy} & \sigma_{zz} \end{bmatrix}. \tag{7}$$

4.3 Edge-Node Meshes

If the input to the algorithm is a triangle (or polygonal) mesh rather than a volume, one must also consider the segmentation relative to the underlying structure of the mesh. So far we have assumed that we are dealing with a mesh created from a volume and that the mesh is "dense," i.e., there are many vertices for each surface region. The watershed algorithm operates on connected nodes in this mesh. However, for tessellated surfaces, the model is frequently sparse, with just enough vertices to define each surface (particularly a problem in planar areas), and some large regions might not contain enough vertices to define a catchment basin with an associated boundary.

This problem can be solved by creating a new mesh, the dual of the original, which has a node for each edge in the original mesh and a connection to each adjacent edge (now nodes) across the faces of the two neighboring triangles (or polygons). This shifts the emphasis of the algorithm from the vertices to the polygons of the mesh. For each edge, i.e., between every pair of vertices, in the original mesh, there is a corresponding node in the new mesh. The curvature of this node is then set as the average of its neighboring vertices' curvatures. After region merging is performed,

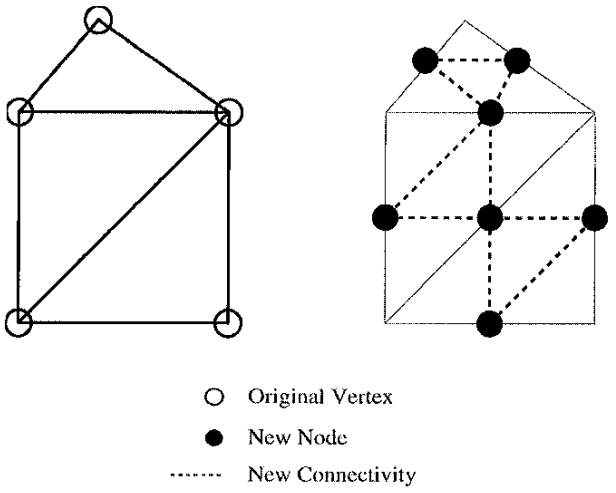

Fig. 9. Creation of edge-based topology based on original mesh.

triangle regions are established, with each triangle being evaluated for region membership based on whether all three of its edges belong to the region in question.

Because the watershed algorithm is independent of how one structures the mesh or computes the height function (or curvature) at each node, a variety of different approximations and preprocessing algorithms can be applied to both the mesh itself and the height function. For instance, an iterative smoothing process could be applied to the height function in order to reduce the effects of noise and approximation errors. Such preprocessing is an area of ongoing investigation and is beyond the scope of this paper.

5 Results

In this section, we present the results of using the watershed algorithm to perform segmentation of surface meshes. We show initial results obtained prior to region merging; examination of these oversegmented solutions demonstrates the need for region merging. The algorithm's capability to successfully segment simple geometric shapes is demonstrated. The performance of the algorithm in the presence of noise is analyzed. The sensitivity of the segmentation to the user-defined threshold is shown. Segmentation results for the edge-node meshes, described in Section 4.3, are then given. Finally, some examples of applications that benefit from the use of this segmentation technique are given, such as mesh reduction and region extraction for CAD models.

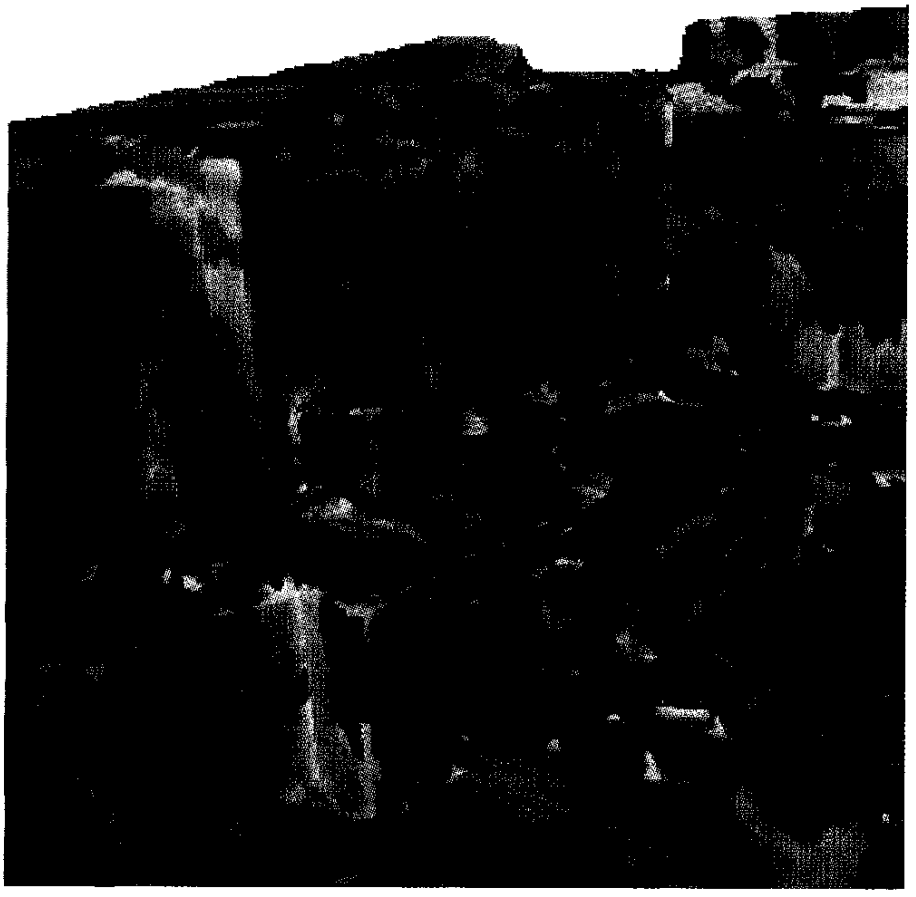

Fig. 10. Oversegmentation resulting from not applying the final region merging step of the algorithm.

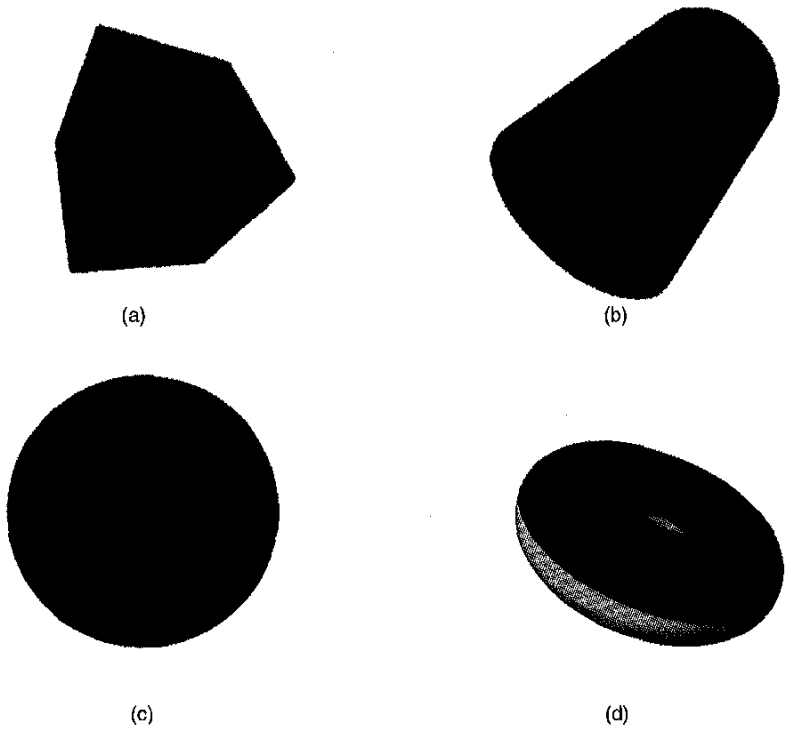

Fig. 11. Segmentation of various test surface types. (a) Cube (six regions), (b) cylinder (three regions), (c) sphere (one region), and (d) torus (two regions).

5.1 Oversegmentation

This section demonstrates the need for region merging by displaying some results obtained without performing the final merging step. As is seen in Fig. 10, the output of the watershed algorithm suffers quite badly from oversegmentation. Any small defects or noise present in the initial model allow the formation of bumps on the surface. If these bumps are concave, they in turn lead to the creation of local minima, which become isolated regions as neighboring vertices flow into them.

5.2 Segmentation of Simple Surfaces

Fig. 11 shows the segmentation results for several analytically defined surfaces with known curvature characteristics. Fig. 11a shows the segmentation of a cube (extracted from a volume), the six faces of which are planar, each separated by a "wall" of high curvature. The high curvature at the edges of the cube allows the algorithm to decompose the surface into the six regions as shown. A similar boundary of high curvature separates the two planar areas at the ends of the cylinder in Fig. 11b. The sphere also has a consistent degree of curvature throughout its surface and is segmented into a single region in Fig. 11c. The torus in Fig. 11d has varying curvature and surface type (it is hyperbolic on the inner hull and elliptic on its outer hull). The curvature also has a pair of maximal loci around the inner and outer hulls that have created the boundary between the two regions as displayed.

5.3 Noise Analysis

This section examines the performance of the algorithm in the presence of additive, uniform noise. For the following analyses, uniform noise is added to the curvature of the vertices as a percentage of the range of curvature for the object, $D_{vertex} = D_{vertex}(X\% \text{ of } (D_{max} - D_{min}))$. Fig. 12 shows how noise affects the segmentations of a torus and a cube. The torus has a relatively constant level of curvature on its surface, whereas the cube has, in effect, zero curvature except at the boundaries between faces. Fig. 12a, Fig. 12b, and Fig. 12c show the torus with varying levels of additive noise applied to the curvature of each vertex. For small levels of noise, 2.5 percent to 5 percent, the boundary between regions moves, but the torus is still segmented into two regions, as appropriate. However, as the noise reaches 10 percent, the partitioning fails dramatically and the torus is oversegmented into 36 regions. At this noise level, the segmentation no longer corresponds to the underlying geometry of the torus. The cube, Fig. 12d, Fig. 12e, and Fig. 12f, displays less sensitivity to small levels of noise. Adding small levels of noise to the boundaries separating the planar faces has negligible effect. As with the torus, once the noise reaches a sufficiently high level, 10 percent, the boundary curvature is no longer significantly higher than the faces and the segmentation breaks down.

5.4 Threshold Sensitivity

The algorithm displays sensitivity to the user-specified threshold encountered in the region merging step. Varying the threshold allows for different levels of segmentation, the

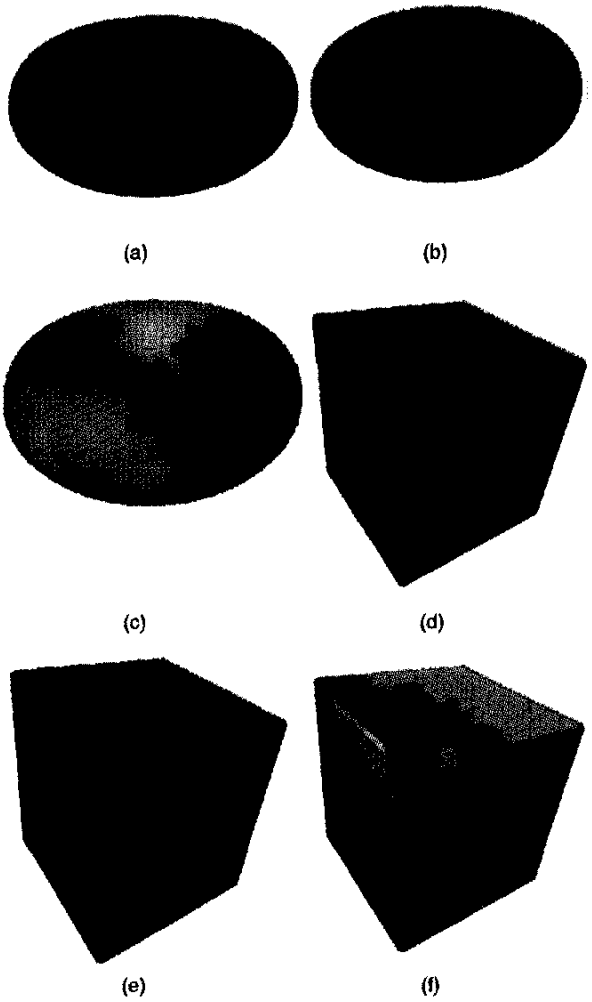

Fig. 12. Torus and cube segmentations with different levels of additive noise applied. (a) Torus, 2.5 percent noise (two regions), (b) torus, 5 percent noise (two regions), (c) torus, 10 percent noise (36 regions), (d) cube, 2.5 percent noise (six regions), (e) cube, 5 percent noise (six regions), (f) cube, 10 percent noise (43 regions).

exact level depending upon the final application. Fig. 14 shows segmentation results for a 3D model of a room that was built by fusing laser range images from different points of view [22]. Because this data is from a sensor, it shows some level of noise. A comparison of results of segmentations using different threshold levels shows that increasing the threshold leads to fewer final regions, as those with successively lower depths are merged with neighboring regions. The boundaries between regions in Fig. 14a represent edges and breaks that are not as highly curved as those in Fig. 14d. There are several areas of interest in the scene that are initially segmented into several pieces, but, as the threshold increases, they are gradually segmented into fewer, more coherent regions. Note how the floor is at first partitioned into multiple areas. The wall partitions, barrels, chairs, and printers (on the lefthand side of the scene) are also partitioned into successively fewer regions.

Fig. 15 shows the segmentation of a dart object, again with several threshold levels. The surface in this case is much simpler than that shown in Fig. 14, yet also displays the same characteristics as the threshold varies.

5.5 Segmentation Based on Mesh Input

All of the segmentation examples thus far have been created using curvature calculated from volumetric inputs as discussed in Section 4.1. Here, we present a segmentation based on surface-based curvature, as described in Section 4.2. The input to the system in this case is a surface mesh rather than a volume. Fig. 16 shows two segmentations of the mug model using different thresholds. This method is capable of generating useful results, but appears to be more prone to high frequency artifacts than segmentations produced from volumetric input. It is possible that these effects could be overcome by applying some type of low-pass filter to the curvature data; we have chosen here to concentrate on the segmentation aspects of the problem and leave this extension of the work for future completion.

5.6 Applications

As mentioned previously, there are several areas that can benefit from this segmentation technique. The advantages of using surface segmentation in two of these areas, mesh reduction and CAD, are highlighted here.

One of the possible applications of the proposed surface segmentation method is improving the results of mesh reduction algorithms. In Fig. 18, we show the results of applying mesh reduction to the dart for various reduction rates. We use an iterative edge-collapse decimation strategy [2], which incorporates a greedy algorithm operating on a

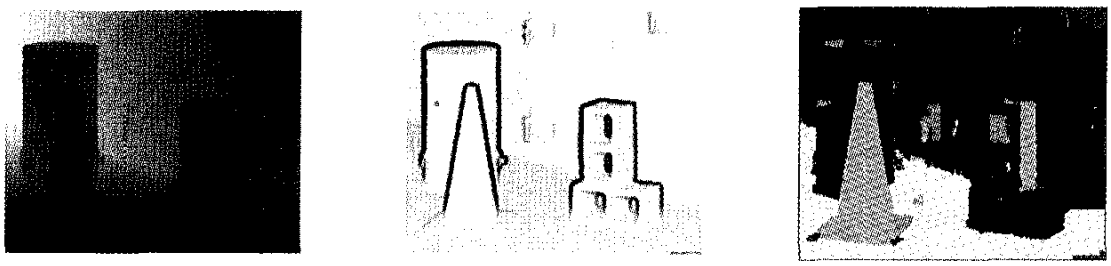

Fig. 13. Example of image segmentation using the watershed algorithm. (a) Input image, (b) gradient magnitude of the input image, smoothed with a Gaussian filter, (c) segmentation of (b) using the watershed algorithm.

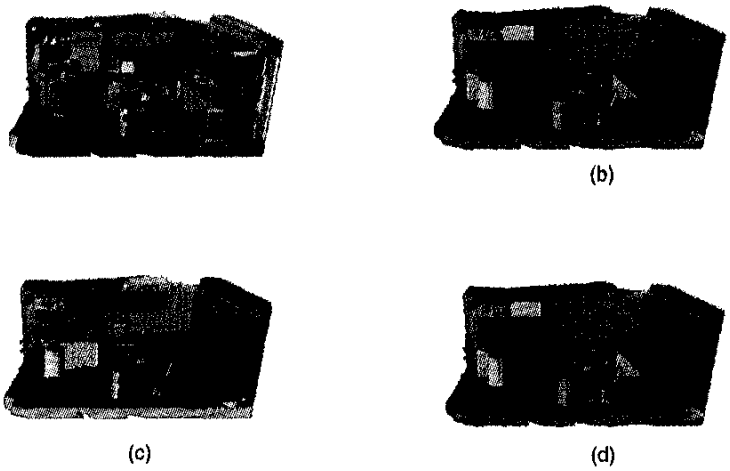

Fig. 14. Segmentation of a scene using varying thresholds, indicated by T. (a) $T = 0.275$ (957 regions), (b) $T = 0.4$ (498 regions), (c) $T = 0.425$ (441 regions), (d) $T = 0.455$ (381 regions).

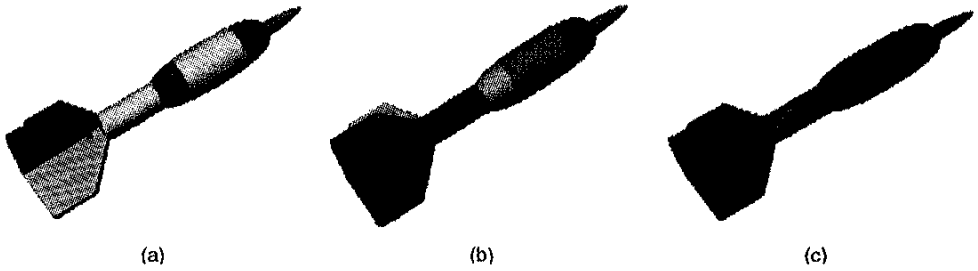

Fig. 15. Dart segmentations. (a) $T = 0.15$ (103 regions), (b) $T = 0.2$ (64 regions), (c) $T = 0.4$ (36 regions).

Fig. 16. Segmentation of the mug model using surface-based curvature calculations. (a) $T = 0.05$ (42 regions), (b) $T = 0.0025$ (126 regions).

curvature metric [23], [24]. Fig. 18a and Fig. 18b show the results of reduction by factors of 50 and 100 respectively. Fig. 18c and Fig. 18d display the improvement possible by specifying the same reduction rates on this surface after it has been segmented. In the latter case, reduction was not allowed across region boundaries, preventing edges between vertices in different regions from collapsing into a

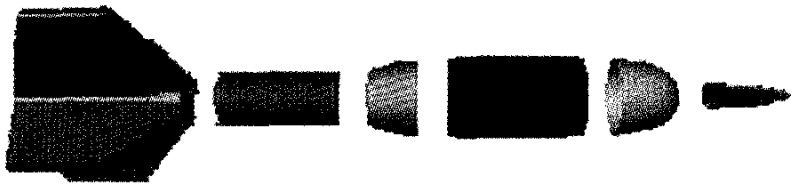

Fig. 17. Several subassemblies of the dart model isolated via region extraction.

single vertex. In this manner, the region boundaries (edges) are preserved.

Another area that can benefit from the use of the segmentation method proposed here is that of computer-aided design. It is possible to read in a general mesh model without any knowledge of its structure save its basic connectivity and segment it and extract any desired regions using the user-specified threshold. Subparts can then be analyzed in detail and the model modified by modifying or deleting assemblies as required. These parts and assemblies can then be added to a database of such parts and recombined and reused in different configurations as needed. A surface mesh can be created using an interactive 3D model generation tool and measurements and specifications for various subassemblies then generated from the segmented model. Fig. 17 shows several parts of the dart extracted from the model as a whole.

6 Conclusions

We have presented here a method of surface segmentation which uses a generalization of watershed regions to 3D meshes. The method can segment either isosurfaces of a 3D volume or surface meshes directly into regions that are bounded by higher curvature. The algorithm displays some sensitivity to the user-specified threshold. Varying the threshold allows for different levels of segmentation, the exact level depending upon the final application.

One aspect of the system that would benefit from future work is the method of calculating curvature for surface meshes. Currently, the results obtained from segmentation of these meshes are prone to high frequency aliasing and

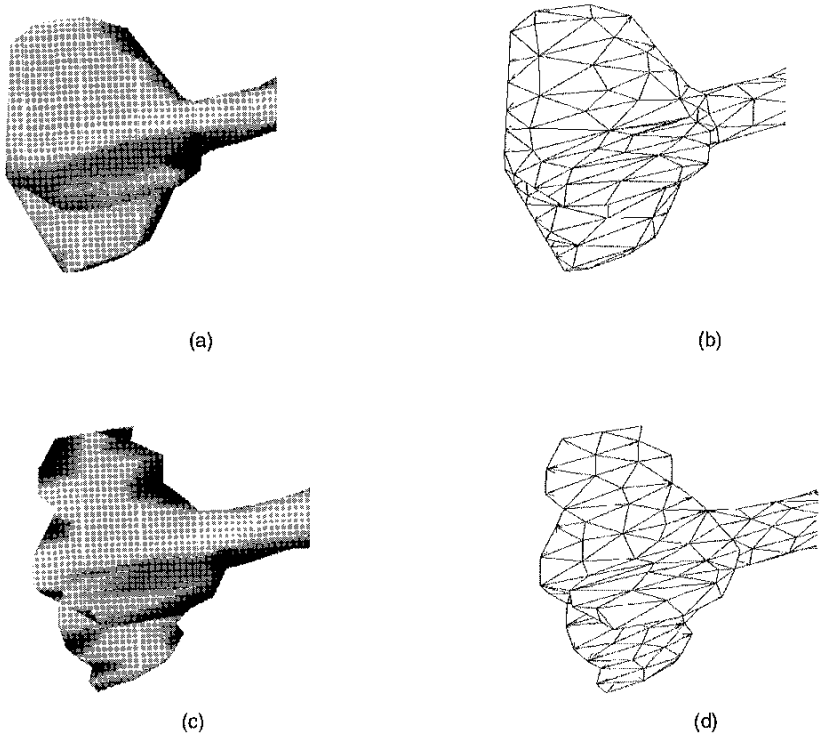

Fig. 18. Mesh reduction on unsegmented and segmented surface. (a) Reduction by a factor of 100 on the unsegmented dart, (b) the vertex connectivity of the unsegmented reduction, (c) reduction by a factor of 100 on the segmented dart, (d) the vertex connectivity of the segmented reduction.

the success of the segmentation depends heavily upon the coarseness of the grid sampling. Smoothing the curvature calculated from these surfaces will, in all probability, improve the segmentation results significantly.

ACKNOWLEDGMENTS

Thanks go to David Breen and the Computer Graphics Group at the California Institute of Technology for providing the dart volume data and to Chris Gourley for providing the mesh reduction code. The image segmentation example was provided by Samuel Burgiss Jr. The range data in Fig. 13a was provided by the Oak Ridge National Laboratory. This work is supported by the U.S. Office of Naval Research Visualization program under grant N00014-97-0227.

REFERENCES

[1] J.P. Serra, *Image Analysis and Mathematical Morphology*. London: Academic Press, 1982.
[2] H. Hoppe, "Progressive Meshes," *Computer Graphics (Proc. SIGGRAPH 96)*, pp. 99-108, July 1996.
[3] A. Varshney, P. Agarwal, and F.P.B. Jr, "Automatic Generation of Multiresolution Hierarchies for Polygonal Models," *Proc. First Workshop Simulation and Interaction in Virtual Environments*, pp. 25-28, 1995.
[4] A.W.F. Lee, W. Sweldens, P. Schröder, L. Cowsar, and D. Dobkin, "MAPS: Multiresolution Adaptive Parameterization of Surfaces," *Computer Graphics (Proc. SIGGRAPH 98)*, pp. 95-104, July 1998.
[5] C.L. Bajaj and T.K. Dey, "Convex Decompositions of Polyhedra and Robustness," *SIAM J. Computing*, vol. 21, pp. 339-364, 1992.
[6] B. Chazelle and L. Palios, "Triangulating a Nonconvex Polytope," *Discrete and Computational Geometry*, vol. 5, pp. 505-526, 1990.
[7] B. Chazelle, D.P. Dobkin, N. Shouraboura, and A. Tal, "Strategies for Polyhedral Surface Decomposition: An Experimental Study," *Proc. 11th Ann. ACM Symp. Computational Geometry*, pp. 297-305, June 1995.
[8] J. Koënderink and A. van Doorn, "The Structure of Two-Dimensional Scalar Fields with Applications to Vision," *Biological Cybernetics*, vol. 33, pp. 151-158, 1979.
[9] D. Eberly, *Ridges in Image and Data Analysis*. Dordrecht: Kluwer Academic, 1996.
[10] R.B. Fisher, A.W. Fitzgibbon, and D. Eggert, "Extracting Surface Patches from Complete Range Descriptions," *Proc. Int'l Conf. Recent Advances in 3-D Digital Imaging and Modeling*, pp. 148-154, Ottawa, Canada, May 1997.
[11] D. Faugeras and M. Hebert, "A 3-D Recognition and Positioning Algorithm Using Geometric Matching between Primitive Surfaces," *Proc. Eighth Int'l Joint Conf. Artificial Intelligence*, pp. 996-1,002, 1983.
[12] P. Besl, *Surfaces in Range Image Understanding*. Springer-Verlag, 1988.
[13] E. Trucco and R.B. Fisher, "Experiments in Curvature-Based Segmentation of Range Data," *IEEE Trans. Pattern Analysis and Machine Intelligence*, vol. 17, no. 2, pp. 177-182, Feb. 1995.
[14] M. Baccar, "Surface Characterization Using a Gaussian Weighted Least Squares Technique towards Segmentation of Range Images," master's thesis, Univ. Tennessee, Knoxville, May 1994.
[15] A.C.F. Colchester, "Network Representation of 2D and 3D Images," *3D Imaging in Medicine*, K.H. Höhne, H. Fuchs, and S. Pizer, eds., pp. 45-62, Springer-Verlag, 1990.
[16] L.D. Griffin, A.C.F. Colchester, and G.P. Robinson, "Scale and Segmentation of Gray-Level Images Using Maximum Gradient Paths," *Image and Vision Computing*, vol. 10, pp. 389-402, 1992.
[17] L.R. Nackerman, "Two-Dimensional Critical Point Configuration Graphs," *IEEE Trans. Pattern Analysis and Machine Intelligence*, vol. 6, no. 4, pp. 442-450, 1984.
[18] J. Koënderink and A. van Doorn, "Local Features of Smooth Shapes: Ridges and Courses," *SPIE Proc. Geometric Methods in Computer Vision II*, vol. 2031, pp. 2-13, 1993.
[19] W.E. Lorensen and H.E. Cline, "Marching Cubes: A High Resolution 3D Surface Construction Algorithm," *Computer Graphics (Proc. SIGGRAPH 87)*, vol. 21, pp. 163-169, July 1987.
[20] J. Koënderink, *Solid Shape*. Cambridge, Mass.: MIT Press, 1991.
[21] J. Sethian, *Level Set Methods: Evolving Interfaces in Geometry, Fluid Mechanics, Computer Vision and Materials Science*. New York: Cambridge Univ. Press, 1996.
[22] R.T. Whitaker, "A Level-Set Approach to 3D Reconstruction From Range Data," *Int'l J. Computer Vision*, vol. 29, pp. 203-231, Oct. 1998.
[23] C. Gourley, "Pattern Vector Based Reduction of Large Multimodal Data Sets for Fixed Rate Interactivity during Visualization of Mutliresolution Models," PhD thesis, Univ. of Tennessee, Knoxville, 1998.
[24] C. Gourley, C. Dumont, and M.A. Abidi, "Fixed-Rate Interactivity for Visualization of Photo-Realistic Multiresolution Models," *Am. Nuclear Soc.: Eighth Topical Meeting on Robotics and Remote Systems*, Apr. 1999.

Alan P. Mangan spent four years in the U.S. Army prior to attending the University of Tennessee, Knoxville. He received his BS degree in electrical engineering in 1996, and MS degree in electrical engineering in 1998. He is currently working as an engineer with Creare, Inc., in Hanover, New Hampshire. He is a member of the IEEE.

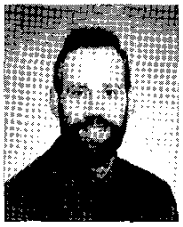

Ross T. Whitaker received his BS degree in electrical engineering and computer science from Princeton University in 1986. He received his PhD in computer science from the University of North Carolina, Chapel Hill, in 1993. In 1994, he joined the European Computer-Industry Research Centre in Munich, Germany, as a research scientist in the User Interaction and Visualization Group. In 1996, he joined the Department of Electrical Engineering at the University of Tennessee as an assistant professor. He teaches image processing, computer vision, and pattern recognition. His research interests include computer vision, image processing, medical imaging, and computer graphics/visualization. He is a member of the IEEE.